Fast flow during current sheet thinning

R. Nakamura,[1] W. Baumjohann,[1] A. Runov,[1] M. Volwerk,[1] T. L. Zhang,[1] B. Klecker,[2]
Y. Bogdanova,[2] A. Roux,[3] A. Balogh,[4] H. Rème,[5] J. A. Sauvaud,[5] and H. U. Frey[6]

Received 30 August 2002; revised 3 October 2002; accepted 4 October 2002; published 14 December 2002.

[1] In this paper we report Cluster observation of a fast flow event in the plasma sheet associated with a small auroral substorm intensification at 1838 UT on August 12, 2001. Cluster, located in the plasma sheet, experienced significant thinning of the current sheet associated with a high-speed Earthward flow of 900 km/s. By using the four spacecraft magnetic field data and a Harris-type current sheet model, it was estimated that the thickness of the current sheet changes from about 1 R_E before the flow observation down to 400 km, i.e., close to the ion inertia length. In the vicinity of this thin current sheet there were also signatures of enhanced current density off the center of the neutral sheet, consistent with recent Geotail results. *INDEX TERMS:* 2760 Magnetospheric Physics: Plasma convection; 2744 Magnetospheric Physics: Magnetotail; 2764 Magnetospheric Physics: Plasma sheet; 2731 Magnetospheric Physics: Magnetosphere—outer. **Citation:** Nakamura, R., et al., Fast flow during current sheet thinning, *Geophys. Res. Lett.*, *29*(23), 2140, doi:10.1029/2002GL016200, 2002.

1. Introduction

[2] Transient fast flows in the near-Earth and midtail plasma sheet are considered to play a key role in magnetotail flux transport processes. These transient flows are observed for different plasma sheet condition: for example, associate with a pseudobreakup during a thinning plasma sheet in the late growth phase [*Nakamura et al.*, 1998], in a thin plasma sheet after substorm onset [*Sergeev et al.*, 1996], in a thick plasma sheet when typical recovery phase signatures are observed [*Sergeev et al.*, 1996; *Baumjohann et al.*, 1999], and at low AE times [*Angelopoulos et al.*, 1992]. The most likely explanation for these fast flows is acceleration in reconnection region tailward of 20 R_E [e.g., *Baumjohann et al.*, 1989, 1999, *Nagai et al.*, 1998].

[3] Formation of a thin current sheet is essential in the energy conversion process during substorms [e.g., *Sergeev et al.*, 1993]. Such thin current sheet structures are thought to lead to plasma instabilities associated with reconnection and current disruption, depending on how thin a current sheet can evolve for a different configurations of the tail. ISEE observations provided evidence of a thin current sheet during the substorm growth phase and the expansion phase [*Sanny et al.*, 1994; *Sergeev et al.*, 1993]. Several studies identified a tail current sheet with peak in the off-equatorial region [*Sergeev et al.*, 1993; *Hoshino et al.*, 1996; *Runov et al.*, 2002] in the near tail as well as the distant tail region. By examining ion and electron distribution functions from Geotail, *Asano* [2001] found a thin current sheet with a strong off-equatorial plane current.

[4] In this paper, we report magnetic field and ion plasma properties obtained by Cluster during a high-speed flow associated with current sheet thinning, which was observed during a small auroral substorm beginning at 1838 UT on August 12, 2001. Cluster, initially located in the plasma sheet observed high-speed flows and several neutral sheet crossings. Using data from four spacecraft we examine the spatial and temporal change of the current sheet during the fast flow.

2. Event Overview

[5] An auroral substorm broke out at 1838 UT identified by the Far Ultraviolet (FUV) instrument [*Mende et al.*, 2000] onboard the IMAGE satellite. Figure 1 shows Wideband Imaging Camera data from FUV taken during a period of 5–10 sec in every 2 minute spin period. The cross in the figure shows the estimated foot point of the satellite from T89 model. The auroral intensification was first detected in the 1838:25 image (Figure 1b) at 0.5 MLT as indicated by the arrow. Aurora expanded westward (Figure 1d) followed by poleward/eastward expansion at 1844:33 UT(Figure 1e), then weakened and moved toward west at 1846:36 UT (Figure 1f).

[6] Cluster was located at $X = -18$, $Y = -6.7$, $Z = 2.3$ R_E in geocentric solar magnetospheric (GSM) coordinates. The relative location of the four spacecraft are shown in Figure 2. SC 1, 2, and 4 are distributed in a plane nearly parallel to the *X-Y* plane within 380 km, SC 3 is located about 1500 km south of the other three, leading them on their traverse from northern to southern lobe.

[7] Cluster observations during the 1838UT auroral substorm are summarized in Figure 3, which shows the spin-resolution (~4 s) data from the fluxgate magnetometer (FGM) experiment [*Balogh et al.*, 2001] and from the Composition and Distribution Function Analyser (CODIF) of the Cluster ion spectrometry (CIS) experiment [*Rème et al.*, 2001]. All the parameters are shown in GSM coordinates. The vertical dashed lines indicate the time of auroral intensification, poleward/eastward expansion, and auroral weakening, respectively.

[8] SC 3 was near the neutral sheet before the auroral activation, whereas the other 3 satellites are in the northern plasma sheet but encountered the neutral sheet after the auroral onset. High-speed Earthward flow took place in association with an enhancement in the B_X for the three northern spacecraft (SC 1, 2, and 4), whereas SC3 encoun-

[1]Institut für Weltraumforschung der ÖAW, Graz, Austria.
[2]Max-Planck-Institut für extraterrestrische Physik, Garching, Germany.
[3]CETP, Velizy, France.
[4]Imperial College, London, UK.
[5]CESR/CNRS, Toulouse, France.
[6]Space Sciences Lab., Berkeley, USA.

0094-8276/02/2002GL016200

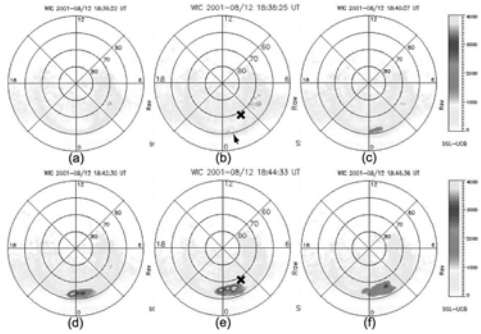

Figure 1. IMAGE/FUV data during the 1838 UT auroral substorm.

tered the southern hemisphere. This indicates a significant steepening of the field gradient in the Z direction due to an enhancement in the current density. Flows are more perpendicular to the magnetic field when the satellites are closer to the neutral sheet as can be seen in the bottom panel, in which the timing of the neutral crossings during the flow interval are marked with small bars at the bottom. Among the three northern spacecraft, SC 2 leads the other two by ~18 s in the initial magnetic field disturbance (indicated by the arrow in the top panel). This time difference corresponds to a dawnward propagation of the disturbance with a speed of ~83 km/s.

3. Orientation of Flow and Current Sheet

[9] The disturbances in B_X and B_Y are well correlated, which suggests a tilt of the field toward the radial direction due to flaring of the tail in the postmidnight sector. We therefore transformed the data into a maximum (minimum) variance coordinate system to eliminate this local time effect. The variance analysis was performed using spin-resolution magnetic field data between 1838 and 1847 UT for each spacecraft independently, yet quite similar results were obtained. Figure 4 shows the proton velocity from SC 1, 3, and 4 and the magnetic field data from the four spacecraft in the new coordinate system. Here we define X', Y', and Z' as the maximum, intermediate, and minimum variance direction, as determined from SC 4. The positive X' axis is tilted toward dusk by 29° in equatorial plane and the Z' axis is tilted by 7° toward midnight in the noon-midnight plane. It can be seen that the high-speed flow as well as field perturbation are aligned with the X' direction. The flow and field disturbance can be divided into three intervals, delineated by the solid lines.

[10] (1) During the first interval, the field traces for each SC are quite different and so are the flow traces, which is

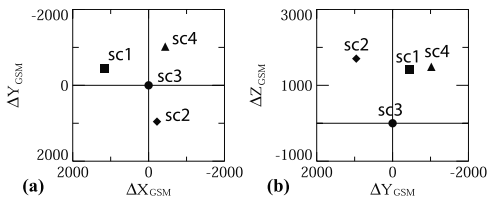

Figure 2. Relative position of the four spacecraft in the (c) X-Y and (d) Y-Z plane.

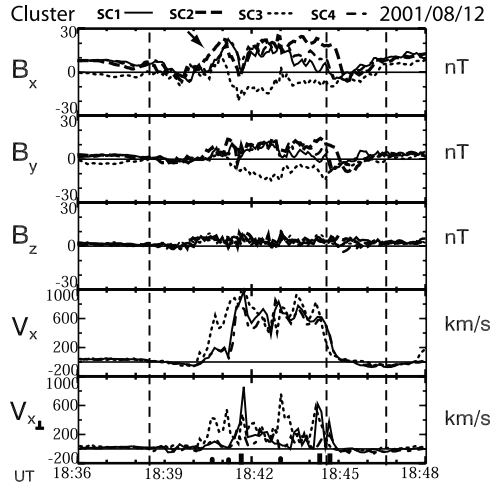

Figure 3. Magnetic field data and X component of the proton velocity between 18:36 and 18:48 UT.

possibly related to the spatial structure of the moving of the high-speed plasma front. The flow at SC 3 is more developed compared to those at SC 1 or 4, which suggests that the flow is more developed near the neutral sheet.

[11] (2) During the second interval, on the other hand, the three flow traces are similar, although the satellites are located at quite different places relative to the neutral sheet. Thus high-speed flow is more spread throughout the plasma sheet.

[12] (3) During the third interval, the three satellites in the northern hemisphere, which are located at nearly the same distance from the neutral sheet, differed significantly in the magnetic field traces. This indicates an enhancement in current density at the three northern spacecraft. On the other hand, the flow traces are similar to that of interval (2).

4. Change in the Structure of the Current Sheet

[13] Since the magnetic field perturbation is predominantly in the X' direction with a very weak Z' component and the flow profile was similar among the satellites at different locations except for interval (1), we fit the data to the Harris current sheet [*Harris*, 1962] to examine quantitatively how the current sheet is structured during the flow interval. In a Harris sheet the magnetic field is represented by $B_X(z) = B_L\tanh(z\text{-}z_0)/L$ where B_L is the lobe field, i.e., field outside the current sheet, z_0 is the location of the neutral sheet and L is the half-thickness of the current sheet. We used simultaneous measurements from three spacecraft to estimate the parameters (z_0, B_L, and L) and compared the estimated B_X^{model} at the location of the fourth spacecraft with the actual data, B_X^{data} to check the validity of the estimation. Here we are interested only in a solution when the difference between B_X^{model} and B_X^{data} does not exceed a factor of 2 and $15 < B_L < 35$ nT. Since the spacecraft spend most of the time, except for the flow interval, in the central plasma sheet where significant current is flowing outside the cluster tetrahedron the latter condition is important to ensure that the model covers a major part of the current sheet up to lobe field, which is expected to be 25–30 nT based on the previous lobe

encounter. We used 30-s averaged data in the model. Various combinations of the three spacecraft were used, but always included the most southern SC3, in the model.

[14] Figure 5 shows the result of the Harris sheet estimation for several sequences before and during the flow interval together with the averaged data. The estimates of z_0, B_L, and B_X^{model} are only shown when the condition discussed above are met. The model results are shown as symbols using the conventional Cluster symbols (rectangle, diamond, and triangle for SC 1, 2, and 4) to represent the spacecraft not used for the modeling but for comparing its data with the model. A reasonable solution also needs the same order of the B_X and Z' values among the three spacecrafts used in the model, i.e., $B_{X\,i} > B_{X\,j} > B_{X\,k}$ when $Z'_i > Z'_j > Z'_k$ (i, j, and k represent the three spacecraft), and larger current density closer to the equator. Hence, good results are mostly concentrated during interval (2). Nonetheless, it can be seen how the current sheet structure changes during the flow event.

[15] Before the onset of the flow, the spatial scale of the current sheet is 5000 km. After southward excursion of the current sheet, during interval (2), the scale reduces to 400 km. Density is reduced by a factor of 2–3 associated with onset of the flow (not shown). Decreased value of density is typically 0.45/cc and the ion-internal length is 340 km during the flow interval (2)–(3), which is comparable to the estimated current sheet half thickness. The maximum current density predicted from the Harris sheet increases up to 39 nA/m^2. Current density determined from the gradient of the B_X using the lower pair of spacecraft, SC 1–3, and the upper one, SC 2–4, are also plotted in the bottom panel of Figure 5. Only positive values are shown when the current sheet orientation allows the assumption of a simple planar current configuration. A similar profile of current density enhancement to the Harris model was obtained from the gradient of the SC1 and SC3, which shows the average current density of 1100 km scale (solid line). On the other hand, the current density obtained by the northern two spacecraft (dotted line), SC 2 and SC 4 separated by 300 km in Z', becomes large during intervals (1) and (3), larger than the current density at SC 1–3 location, which are closer to the equatorial plane. This suggests that the current density has a peak at the off-equatorial location during intervals (1) and (3).

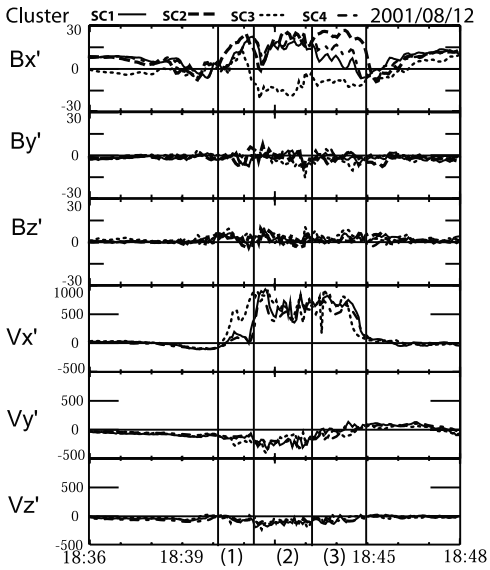

Figure 4. Magnetic field and ion plasma data in maximum variance coordinates (see details in text).

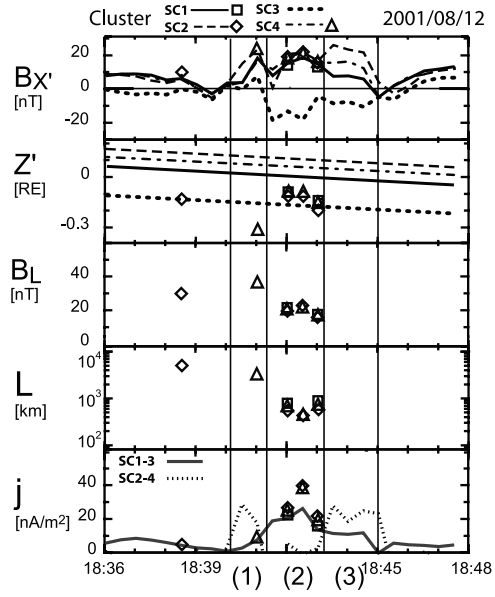

Figure 5. X component of the magnetic field, current sheet location, lobe field, and half thickness of the current sheet and the current density. The curves in the top two panels are data while the symbols are the results from the Harris current sheet model. The curves in the bottom plot shows the current density obtained by the two pairs of SC.

5. Discussion

[16] Cluster located at 1.4 MLT (T89 model foot point location 2.1 MLT) observed the flow disturbance about 2.5 ± 1 min later than the auroral activation which took place at 23.7–0.7 MLT. By taking into account the dawnward propagation speed (83 km/s) observed at Cluster as the propagation speed of the flow disturbance in the azimuthal direction, the Earthward flow and the aurora activations are very likely to be linked, as was also shown in previous studies [*Fairfield et al.*, 1999; *Nakamura et al.*, 2001].

[17] Determination of the current sheet thickness is important for understanding the possible instabilities responsible for substorms. Here we obtained a clear thinning of the plasma sheet/current sheet closely related to the high-speed flows. Such thin current sheets have been observed by the ISEE satellite pair during substorm growth phase and expansion phase [*Sanny et al.*, 1994; *Sergeev et al.*, 1993, 1998]. The maximum current density of 39 nA/m obtained in this study is comparable to that obtained by *Sergeev et al.* [1998].

[18] Interesting to note that the thin current sheet associated with the fast flow is surrounded by a current layer with larger current density in the off-neutral sheet region, a signature expected in a bifurcated current sheet. Such bifurcated current sheet was predicted in the simulation at the outflow part near the reconnection region associated with formation of a shock-like structure [i.e., *Hoshino et al.*,

1998]. Geotail ion and electron distribution functions and moments in the midtail region also showed that a thin current sheet involves a bifurcated structure due to the ion kinetic behavior, which will lead to an electron dominated current layer off the equatorial plane [*Asano*, 2001]. The observed current sheet profile, therefore, suggests that Cluster approached the vicinity of the ion diffusion region associated with the reconnection process. From the B_X and Z' profile in Figure 5 we can deduce that the three upper spacecraft was located 900 ± 300 km off the neutral sheet during phase (3), which represents the scale-size of the bifurcated current sheet. Since the spatial resolution of the current density observation by Cluster is limited by the spatial separation of the spacecraft, whether the current sheet 400 km scale involves further bifurcated part inside must await study during the later mission phase when the tetrahedron-scale is becoming less than 500 km. Bifurcated current was observed not only associated with high-speed transient flows during substorm intensification but also during recovery phase in the midtail [*Runov et al.*, 2002] and is a quite common signature in the distant tail [*Hoshino et al.*, 1996], suggesting its importance for understanding the dynamics of the tail current sheet.

6. Conclusion

[19] The plasma sheet fast flow during the auroral beginning at 1838UT, August 12, 2001 was directly related to the thinning of the current sheet from a typical scale of 1 R_E to 400 km, which is comparable to the ion inertial length. The observation is consistent with recent Geotail observations of a thin current sheet which involves a bifurcated structure due to the ion kinetic behavior. In fact, Cluster with four spacecraft detected a thin Harris-type current sheet is surrounded by a bifurcated current, which possibly shows the structure of the current sheet related to the reconnection process.

[20] **Acknowledgments.** We thank V. A. Sergeev, M. Hoshino, T. Nagai for helpful discussions and comments. The authors are grateful to H. Eichelberger, G. Laky, G. Leistner, E. Georgescu for helping Cluster data analysis. We acknowledge CSDS, GCDC, ACDC making available the data used in this study. The August 12, 2001, event was selected as Event A in the Substorm Onset session in the Cluster March 2002 workshop. We thank H. Laakso and the workshop participants for their helpful comments.

References

Angelopoulos, V., et al., Bursty bulk flows in the inner central plasma sheet, *97*, 4027, 1992.

Asano, Y., Configuration of the thin current sheet in substorms, Ph.D. thesis, Univ. Tokyo, 2001.

Balogh, A., et al., The Cluster magnetic field investigation: overview of in-flight performance and initial results, *Ann. Geophys.*, *19*, 1207, 2001.

Baumjohann, W., G. Paschmann, and C. A. Cattell, Average plasma properties in the central plasma sheet, *94*, 6597, 1989.

Baumjohann, W., M. Hesse, S. Kokubun, T. Mukai, T. Nagai, and A. A. Petrukovich, Substorm dipolarization and recovery, *104*, 24,995, 1999.

Fairfield, D. H., et al., Earthward flow bursts in the inner magnetotail and their relation to auroral brightenings, AKR intensifications, geosynchronous particle injections and magnetic activity, *104*, 355, 1999.

Harris, E. G., On a plasma sheath separating regions of oppositely directed magnetic field, *Nuovo Cimento*, *23*, 115, 1962.

Hoshino, M., et al., Structure of plasma sheet in magnetotail: Double-peaked electric current sheet, *101*, 24775, 1996.

Hoshino, M., et al., Ion dynamics in magnetic reconnection: Comparison between numerical simulation and Geotail observations, *J. Geophys. Res.*, *103*, 4509, 1998.

Mende, S. B., et al., Far ultraviolet imaging from the IMAGE spacecraft, *Space Sci. Rev.*, *91*, 287, 2000.

Nagai, T., et al., Structure and dynamics of magnetic reconnection for substorm onsets with Geotail observations, *103*, 4419, 1998.

Nakamura, R., et al., Temporal and spatial relationships between midtail substorm disturbance and auroral substorm onset, in "SUBSTORMS-4", Terra Sci. Pub./Kluwer Acad. Pub., pp. 179, 1998.

Nakamura, R., et al., Flow bursts and auroral activations: Onset timing and foot point location, *J. Geophys. Res.*, *106*, 10,777, 2001.

Rème, H., et al., First multispacecraft ion measurements in and near the Earth's magnetosphere with the identical Cluster ion spectrometry (CIS) experiment, *Ann. Geophys.*, *19*, 1303, 2001.

Runov, A., et al., Cluster Observations of a bifurcated current sheet, *Geophys. Res. Lett.*, in press, 2002.

Sanny, J., et al., Growth-phase thinning of the near-Earth current sheet during the CDAW 6 substorm, *J. Geophys. Res.*, *99*, 5805, 1994.

Sergeev, V. A., et al., Structure of the tail plasma/current sheet at 11 RE and its changes in the course of a substorm, *J. Geophys. Res.*, *98*, 17,345, 1993.

Sergeev, V. A., et al., Detection of localized, plasma-depleted flux tubes or bubbles in the midtail plasma sheet, *J. Geophys. Res.*, *101*, 10,817, 1996.

Sergeev, V., et al., Current sheet measurements within a flapping plasma sheet, *J. Geophys. Res.*, *103*, 9177, 1998.

W. Baumjohann, R. Nakamura, A. Runov, M. Volwerk, and T. L. Zhang, IWF der ÖAW, Schmiedlstr. 6, A-8042, Graz, Austria. (rumi@oeaw.ac.at)

Y. Bogdanova and B. Klecker, Max-Planck-Institut für extraterrestrische Physik, Postf. 1312 Garching, D-85741, Germany.

A. Roux, CETP, 10/12 Avenue de L'Europe, F-78140,Velizy, France.

A. Balogh, Imperial College, London, SW7 2BZ, UK.

H. Rème and J. A. Sauvaud, CESR/CNRS, 9 Ave. du Colonel Roche, B.P. 4346, F-31028 Toulouse Cedex 4, France.

H. U. Frey, SSL, Univ. California, Berkeley, CA 94720-7450, USA.